

## Novel Integration of Ultra-thin Al<sub>2</sub>O<sub>3</sub> with Low-*k* Dielectric as Bi-layer Liner for Capacitance Optimization and Stress Mitigation in Cu-TSV

Lin Zhang<sup>1,2,\*</sup>, Hongyu Li<sup>1</sup>, Yang Shang<sup>2</sup>, Woosik Yoo<sup>3</sup>, Hao Yu<sup>2</sup>, and Chuan Seng Tan<sup>2</sup>

<sup>1</sup>Institute of Microelectronics, A\*STAR, Singapore 117685; <sup>2</sup>Nanyang Technological University, Singapore 639798; <sup>3</sup>WaferMasters, Inc, San Jose, CA 95112, USA. \*E-mail: zhang.lin@ntu.edu.sg

### Abstract

A bi-layer liner is integrated in Cu-TSV for capacitance optimization and stress mitigation. Low-*k* (SiOC) liner with smaller elastic modulus is integrated in TSV and lower stress is exerted on the surrounding Si compared with PETEOS. It also reduces the TSV capacitance by ~26%. Thin Al<sub>2</sub>O<sub>3</sub> is inserted between low-*k* liner and Si substrate to induce negative fixed charge ( $Q_f = -1.3 \times 10^{12} \text{cm}^{-2}$ ). This causes flat-band voltage shift ( $\Delta V_{FB} = +19\text{V}$ ) and the TSV is operated in the stable accumulation region hence immune to spatial variation due to hot-spot heating.

### 1. INTRODUCTION

TSV allows “orthogonal scaling” in the next generation of integrated circuits and systems for performance growth and functional diversification. TSV is fabricated by deep silicon etching, lining with dielectric and filling with Cu [1] hence forming a MOS structure [2]. Cu-TSV exerts thermo-mechanical stress on Si due to CTE mismatch which results in mobility variation [3] and interconnect distortion [4]. In addition, TSV parasitic capacitance has predominant impact on the circuit operation [5]. The depletion capacitance ( $C_{dep}$ ) is susceptible to and increases with temperature. The fluctuation in  $C_{dep}$  and the impact on TSV signal delay is calculated using a predictive technology model (PTM) in Fig. 1(a)(b). When TSV is operated in the depletion region (~0-5 V),  $C_{dep}$  dependence on temperature results in spatial TSV latency variation and clock skew in H-tree network in the event of non-uniform hot-spot heating (Fig. 1(c)). Therefore, TSV with tolerance to spatial variation is desirable for robust 3DIC design. TSV capacitance is stable with temperature if one operates it in the accumulation region ( $C_{ox}$ ). As  $C_{ox}$  is higher than  $C_{dep}$ , one needs to keep the capacitance <100 fF for final application [6].

One solution to TSV stress and capacitance issues is to use low-*k* dielectric liner with lower elastic modulus [7] and permittivity [8]. Flat-band voltage ( $V_{FB}$ ) shift is achieved by including negative fixed charge at the *p*-Si/liner interface with a thin layer of Al<sub>2</sub>O<sub>3</sub> such that the TSV operates at stable  $C_{ox}$  [9]. In this paper, we are presenting this novel integration of ultra-thin Al<sub>2</sub>O<sub>3</sub> with low-*k* dielectric as bi-layer liner in Cu-TSV.

### 2. TSV FABRICATION

Three sets of TSV structures ( $\phi=5 \mu\text{m}$ , aspect ratio =1:3) are fabricated on 8" *p*-Si wafer. This aspect ratio is chosen for ease of fabrication and is sufficient to study the properties of

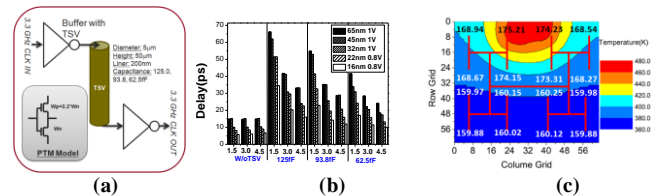


Fig.1. (a) TSV signal delay estimation using predictive technology model (PTM) for different capacitance; (b) Comparison of TSV signal delay for different technology node, *n*-MOSFET width ( $W_n$  in  $\mu\text{m}$ ) and TSV capacitance (fF); (c) H-tree clock skew (ps) due to non-uniform hot-spot heating and the corresponding spatial variation in TSV capacitance.

the liner. The TSV fabrication process is similar to that reported in [10]. Thin Al<sub>2</sub>O<sub>3</sub> layer (~10 nm) is deposited in one set of TSV structures by atomic layer deposition (ALD) process at a temperature <400 °C, followed by a Black Diamond low-*k* liner (~200 nm) deposition which is carried out in a PECVD chamber at 350 °C. Hence the bi-layer liner is formed. The other two sets of TSV structures have PETEOS liner (~200 nm) deposited at 400 °C and Black Diamond low- $\kappa$  liner (~200 nm) deposited, respectively, as control samples.

### 3. RESULTS AND DISCUSSION

#### Fabrication Process Results

A void-free Cu filled TSV with a combination of Al<sub>2</sub>O<sub>3</sub> and low-*k* bi-layer liner is shown in Fig. 2. TEM and EDX analysis result in Fig. 2 show the chemical composition of Si, Al<sub>2</sub>O<sub>3</sub>, low-*k* and Cu, and also confirms that the Al<sub>2</sub>O<sub>3</sub>/low-*k* bi-layer is successfully and conformally integrated as the TSV liner with an average thickness of ~200 nm. The fabrication results of the other two sets of TSV structures with pure PETEOS oxide liner and pure low-*k* liner are reported previously in [11] and [12].

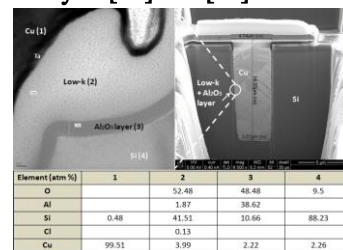
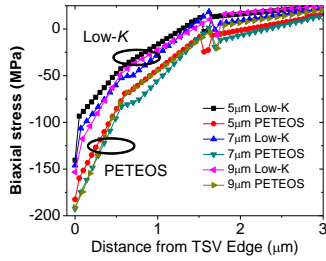


Fig. 2. FIB image of TSV and TEM close-up view of the liner stack.

#### Stress Modeling and Measurement

Finite element analysis in Fig.3 shows that low-*k* liner, with smaller elastic modulus (~7.2GPa), acts as a compliant layer to cushion the Cu-TSV stress on Si compared with PETEOS (75GPa). High resolution Raman spectroscopy is used to verify the biaxial stress exerted on Si. In Fig. 4(a), it is verified that with low-*k* liner, lower compressive stress is exerted by Cu-TSV on the Si between the TSV. This has

positive implication on variability, reliability and keep-out zone. The 2D stress map is presented in Fig. 4(b).



**Fig. 3.** (FEA Simulation) Thermo-mechanical stress exerted by a single Cu-TSV on Si as a function of distance from the edge of TSV.

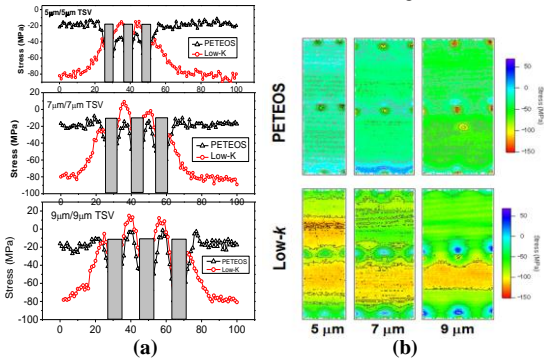


**Fig. 4.** (a) Si Stress profile (biaxial) along TSV rows from Raman Measurement ( $\lambda = 488$  nm). Each row contains 3 TSV with similar TSV pitch and diameter (5, 7, 9  $\mu\text{m}$ ). The stress profiles show that low-k liner is more compliant and can cushion stress exerted by Cu-TSV on the Si (between TSV) more effectively than PETEOS oxide; (b) Biaxial stress mapping of the Si based on micro-Raman spectroscopy.

#### Electrical Measurement Results

The measured CV curves at 100 kHz on TSV structures with PETEOS oxide liner, low- $k$  liner and  $\text{Al}_2\text{O}_3/\text{low-}k$  bi-layer liner after annealing in forming gas ( $\text{N}_2/\text{H}_2$ ) at 350 °C for 30min are shown in the Fig. 5(a). It is shown that by replacing the PETEOS oxide liner with the low- $k$  liner which has an estimated dielectric constant of  $\sim 2.8$ , the accumulation capacitance is reduced by  $\sim 26\%$ . As discussed in [11] and [13], fixed charge ( $Q_f$ ) can effectively shift the  $V_{\text{FB}}$ . Due to the insertion of  $\sim 10$  nm thin  $\text{Al}_2\text{O}_3$  layer between Si and the low- $k$  liner, a large amount of negative fixed charge is induced at the liner/Si interface and the charge density is on the order of  $\sim -1.3 \times 10^{12} \text{ cm}^{-2}$ . The negative fixed charge causes a positive shift in  $V_{\text{FB}}$  ( $\Delta V_{\text{FB}} = +19\text{V}$ ). As a result, TSV is operated in the stable accumulation capacitance region within the voltage of interests ( $\sim 0\text{-}5$  V) to overcome the spatial performance variation caused by non-uniform hotspot heating.

The effect of annealing on  $\text{Al}_2\text{O}_3/\text{low-}k$  liner is presented in Fig. 5(b) and the  $k$  value remains constant. With the insertion of  $\text{Al}_2\text{O}_3$ , the TSV is operated in the stable accumulation region between 0-5V and does not fluctuate with temperature (25 to 100°C) as shown in Fig. 5(c). Similar to [13], the stability of  $\text{Al}_2\text{O}_3$ -induced negative fix charge is also studied under prolonged biasing with a high electric field of 2 MV/cm. The result in Fig. 5(d) confirms that sufficient negative fixed charge is maintained even under electric field biasing.

IV measurement is performed and Fig. 6 presents the

leakage current density of  $\text{Al}_2\text{O}_3/\text{low-}k$  bi-layer liner at an electric field of 2 MV/cm after annealing at various conditions. The result shows that annealing in forming gas at 350 °C for 2 hours or at 400 °C for 0.5 hour can significantly improve the leakage current and effectively reduce the leakage current density to a level of  $\sim 4 \times 10^{-6} \text{ A/cm}^2$  at mid-distribution, comparable with that of PETEOS liner.

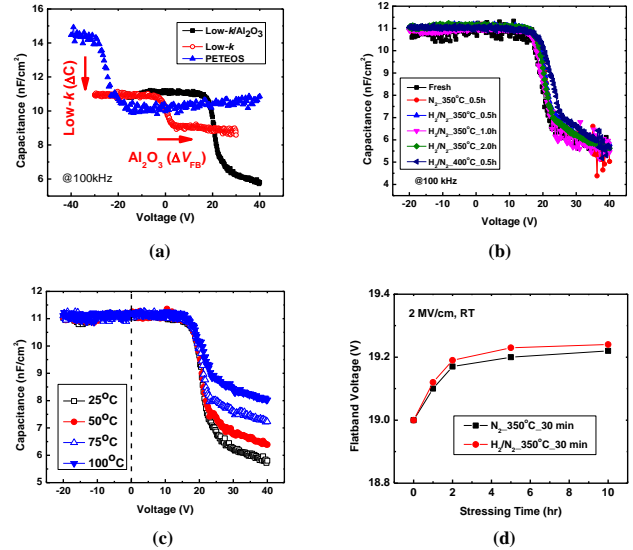


**Fig. 5.** (a) CV characteristics of TSV structures with different liners after annealing in forming gas ( $\text{N}_2/\text{H}_2$ ) at 350 °C for 30min; (b) CV characteristics of TSV with  $\text{Al}_2\text{O}_3/\text{low-}k$  liner after annealing at various conditions; (c) Stable accumulation capacitance within operating voltage of interest (0-5V) is achieved; (d) The stability of the negative fixed charge under 2 MV/cm biasing. The  $V_{\text{FB}}$  increases initially and stabilizes after 5 hours.

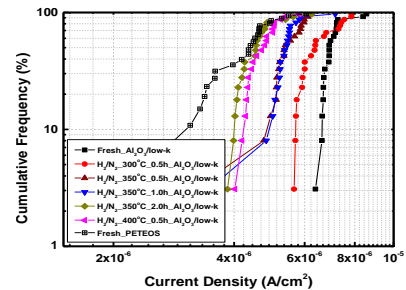


**Fig. 6.** IV measurement of  $\text{Al}_2\text{O}_3/\text{low-}k$  bi-layer liner after annealing. Leakage current density is improved to a level comparable with PETEOS oxide liner after annealing in forming gas ( $\text{N}_2/\text{H}_2$ ) at 350 °C for 2 hours or at 400 °C for 0.5 hour.

#### 4. CONCLUSION

A novel material integration of thin  $\text{Al}_2\text{O}_3$  with low- $k$  bi-layer in the TSV structure as the liner has been successfully achieved and used to reduce TSV stress and a  $\sim 26\%$  reduction in capacitance is obtained. Negative fixed charge induced in the thin  $\text{Al}_2\text{O}_3$  layer causes positive flat-band voltage shift. TSV is operated in the stable accumulation region hence immune to spatial temperature variation.

#### References

- [1] S. Ramaswami, et al, *IEEE TDMR*, 2009. [2] T. Bandyopadhyay, et al, *IEEE 3DIC*, 2009. [3] A. Mercha, et al, *IEDM*, 2010. [4] J.C. Lin et al, *IEDM*, 2010. [5] G. Katti, et al, *TED*, 2010. [6] Liu et al, *IEDM*, 2008. [7] P.S. Ho, et al, *JAP*, 2003. [8] R.J. Hoofman, et al, *IITC*, 2005. [9] L. Zhang, et al, *IEDM*, 2011. [10] A. Yu, et al, *ECTC*, 2009. [11] L. Zhang, et al, *IEEE EDL*, 2011. [12] L. Zhang, et al, *JJAP*, 2012. [13] L. Zhang, et al, *IEEE EDL*, 2012.